processes

MDPI

Article

The Crack Propagation Behaviour of CO_2 Fracturing Fluid in Unconventional Low Permeability Reservoirs: Factor Analysis and Mechanism Revelation

Qiang Li [1,3,4], Qingchao Li [2,3,4,*], Hongqi Cao [1], Jingjuan Wu [2], Fuling Wang [1,*] and Yanling Wang [3,4]

[1] Faculty of Engineering, China University of Petroleum-Beijing at Karamay, Karamay 834000, China; liqiang@s.upc.edu.cn (Q.L.); caohq@st.cupk.edu.cn (H.C.)
[2] School of Energy Science and Engineering, College of Materials Science and Engineering, Henan Polytechnic University, Jiaozuo 454000, China; wujj2020@hpu.edu.cn
[3] College of Petroleum Engineering, China University of Petroleum (East China), Qingdao 266580, China; wangyl@upc.edu.cn
[4] Key Laboratory of Unconventional Oil & Gas Development (China University of Petroleum (East China)), Ministry of Education, Qingdao 266580, China
* Correspondence: liqingchao2020@hpu.edu.cn (Q.L.); wangfl@cupk.edu.cn (F.W.)

Abstract: To circumvent the numerous deficiencies inherent to water-based fracturing fluids and the associated greenhouse effect, CO_2 fracturing fluids are employed as a novel reservoir working fluid for reservoir reconstruction in unconventional oil fields. Herein, a mathematical model of CO_2 fracturing crack propagation based on seepage–stress–damage coupling was constructed for analysing the effects of different drilling fluid components and reservoir parameters on the crack propagation behaviour of low permeability reservoirs. Additionally, the fracture expansion mechanism of CO_2 fracturing fluid on low permeability reservoirs was elucidated through mechanical and chemical analysis. The findings demonstrated that CO_2 fracturing fluid can effectively facilitate the expansion of cracks in low-permeability reservoirs, and thickener content, reservoir pressure, and reservoir parameters were identified as influencing factors in the expansion of reservoir cracks and the evolution of rock damage. The 5% CO_2 thickener can increase the apparent viscosity and fracture length of CO_2 fracturing fluid to 5.12 mPa·s and 58 m, respectively, which are significantly higher than the fluid viscosity (0.04 mPa·s) and expansion capacity (13 m) of pure CO_2 fracturing fluid. Furthermore, various other factors significantly influence the fracture expansion capacity of CO_2 fracturing fluid, thereby offering technical support for fracture propagation in low-permeability reservoirs and enhancing oil recovery.

Keywords: unconventional shale reservoirs; CO_2 fracturing fluid; reservoir fracture propagation; enhanced oil recovery

check for updates

Academic Editor: Qingbang Meng

Received: 24 December 2024
Revised: 1 January 2025
Accepted: 6 January 2025
Published: 8 January 2025

Citation: Li, Q.; Li, Q.; Cao, H.; Wu, J.; Wang, F.; Wang, Y. The Crack Propagation Behaviour of CO_2 Fracturing Fluid in Unconventional Low Permeability Reservoirs: Factor Analysis and Mechanism Revelation. *Processes* **2025**, *13*, 159. https://doi.org/10.3390/pr13010159

Copyright: © 2025 by the authors. Licensee MDPI, Basel, Switzerland. This article is an open access article distributed under the terms and conditions of the Creative Commons Attribution (CC BY) license (https://creativecommons.org/licenses/by/4.0/).

1. Introduction

The pursuit of economic development inevitably entails a concomitant increase in energy consumption and environmental pollution [1,2]. However, these factors provide a tangible material guarantee for the quality of life of the general population [3]. Nevertheless, the damage to the natural environment and the scarcity of energy resources have become crucial factors supporting economic growth and social stability [4,5]. Scientists have initiated research into key strategies for effectively managing the virtuous cycle between the ecological environment and energy replenishment. The current approach to addressing

energy shortages primarily entails the efficient exploration of new energy sources and the significant advancement of unconventional fossil energy [6,7]. (1) New energy materials and energy forms: the existence of alternative energy sources, including wind, hydrogen, solar and tidal energy, has gradually attracted the attention of scientists, offering significant potential for the efficient replacement of traditional energy sources. Furthermore, the diversity of energy sources provides a means of effectively selecting different special application scenarios, offering a substantial prospect for enhancing energy utilisation efficiency and efficient production [8,9]. Nevertheless, the low collection efficiency of emerging energy sources, including tidal, wind, and solar energy, is insufficient to supplant traditional energy sources. Concurrently, the limited energy storage capacity of equipment utilised for these energy sources has also impeded the accelerated development and pervasive promotion of the new energy industry [10]. Consequently, the strategy of replacing traditional energy sources with new energy still presents numerous challenges and obstacles that must be addressed. (2) Unconventional fossil energy: shale energy, an abundant fossil resource in unconventional reservoirs, is widely regarded by petroleum engineers as a critical alternative or supplementary energy source for efficient extraction and development [11,12]. Furthermore, the abundance of shale deposits and their extensive distribution have become key geological advantages of shale energy, currently attracting significant attention [13]. Numerous reservoir transformation techniques, including acidification [14], fracturing [15], and the reduction in sand-bearing or heavy oil viscosity [16,17], can be employed for the transformation of deep shale reservoirs. Nevertheless, the water–wet interface of the shale reservoir can readily form intermolecular hydrogen bonds with water molecules in the oilfield working fluid, which results in the formation of a robust water-sensitive phenomenon on the shale surface [18,19]. The water-sensitive phenomenon will reduce reservoir rock permeability and oil recovery [20]. Thus, the reservoir transformation measures typically employed in conventional oil reservoirs are not wholly applicable to the oil production of unconventional shale reservoirs.

Fracturing technology is a widely employed method for reservoir transformation across various geological settings [21,22]. Its numerous advantages, including low cost, efficient fracture propagation, and minimal reservoir pollution, have established it as a critical approach for enhancing resource recovery [23]. Water-based fracturing [22], oil-based fracturing [24], foam fracturing [25], and clean fracturing technologies [26] are currently applied to specific fracturing scenarios based on their fluid characteristics and the geological structure of the reservoirs. Water-based fracturing fluids exhibit relatively greater geological versatility, enabling effective crack propagation and rock deformation in most geological reservoirs [27]. However, water contamination and reservoir blockage caused by cross-linking agents in water-based fracturing fluids have emerged as significant bottlenecks limiting their widespread application [28,29]. Additionally, the water-sensitive effects induced by water-based fracturing fluids can further reduce reservoir permeability, posing challenges to their efficiency in certain conditions. The foam in foam-based fracturing fluid is susceptible to degradation caused by variations in reservoir temperature or pressure, which significantly affects the fluid stability of the fracturing system [30]. Furthermore, alterations in foam morphology or foam rupture result in changes to the properties of the fracturing fluid, including fluid viscosity, filtration loss, and sand-carrying capacity [31,32]. Oil-based fracturing fluids effectively mitigate the water-sensitive effects associated with water-based fracturing fluids on reservoir rocks, thereby reducing rock expansion and preventing permeability decline [33,34]. Additionally, oil-based fracturing fluids do not pose a risk of contaminating reservoir groundwater and can be recovered along with crude oil during post-fracturing production. However, numerous challenges such as difficult to control fluid viscosity, limited sand-carrying capacity, and high operational costs have

significantly hindered the widespread adoption of oil-based fracturing fluids in oilfield applications. The utilisation of CO_2 fracturing fluid has emerged as a pivotal research domain for petroleum engineers [35,36], and the gradual attenuation of the greenhouse effect is anticipated as a consequence of the pervasive deployment of CO_2 fracturing fluid. However, the application of CO_2 fracturing fluids in reservoir transformation still faces several challenges, including issues related to fluid viscosity [37], fracture propagation, and sand-carrying capacity, among others, that require resolution. Various measures have been investigated and are gradually being implemented to address these limitations. CO_2 thickeners, including fluorine-containing, hydrocarbon, and siloxane [38], can be employed to enhance the viscosity of CO_2 fracturing fluid. The siloxane thickeners that have been subjected to preliminary evaluation have demonstrated remarkable CO_2 thickening capabilities. Fluorinated thickeners can achieve a thickening capacity of 4.5 mPa·s for CO_2 fracturing fluid at a 1% content, but their greater solubility in groundwater increases groundwater pollution and production costs. Although hydrocarbon thickeners can achieve a thickening capacity of 1.3 mPa·s for CO_2 fracturing fluid at 5% content without the need for co-solvents, a larger addition amount increases the cost of using hydrocarbon thickeners. Siloxane thickener has been shown to achieve a thickening capacity of 4.5 mPa·s for CO_2 fracturing fluid at a 2% content, thus demonstrating superior performance in comparison to the aforementioned two thickeners. Another critical challenge for CO_2 fracturing fluids is the need to investigate the efficiency and mechanisms of fracture propagation in reservoirs [39]. However, limited attention has been given to analysing fracture propagation efficiency or the influence of reservoir geological characteristics, presenting a significant challenge to the broader application of CO_2 fracturing technology. The extremely low viscosity and large filtration loss of CO_2 fracturing fluid also hinder the expansion behaviour of this type of fracturing technology in reservoir fractures. Nevertheless, it is important to note that CO_2 fracturing fluid, akin to water-based fracturing technology, can utilise numerical simulations to explore the expansion laws of unconventional fractures. Simultaneously, the performance evaluation of CO_2 fracturing technology has the potential to provide the necessary data support for the efficient exploitation of unconventional shale resources and to address the issue of groundwater pollution.

Herein, this paper established the seepage–stress–damage coupling equation and employs the extended finite element fracture extension mathematical model to analyse the flow, seepage and fracture extension ability of CO_2 fracturing fluid in reservoir fractures. Concurrently, the cohesive unit damage criterion was employed to examine the cracking and damage progression of reservoir rocks. Ultimately, the mechanical analysis and interaction of microscopic molecules elucidated the expansion mechanism of CO_2 fracturing fluid on reservoir fractures. The objective of this study is to provide a foundation for the advancement of CO_2 fracturing technology and the optimal utilisation of unconventional reservoirs.

2. Materials and Methods

2.1. Mathematical Model of Fluid–Solid Damage Coupling Between CO_2 and Reservoir Rock

The seepage field control equation (Equation (1)) considers that the physical properties of CO_2 are constructed by summarising rock deformation, continuity equation, and Darcy's law, which can be used to reveal the seepage law of CO_2 fracturing fluid in reservoir rocks [40].

$$\frac{\partial \rho P}{\partial t} = \nabla \cdot \left(\frac{\rho k}{\mu} \nabla P \right), \tag{1}$$

where t is time, s. μ is the viscosity of CO_2 fracturing fluid, mPa·s. k presented the permeability of reservoir rock, μm^2. ρ is the density of CO_2 fracturing fluid, $kg \cdot m^{-3}$. σP is

the pressure difference, MPa. Equation (1) can be used to analyse the seepage and filtration capacity of CO_2 fracturing fluid in reservoir rocks and fractures. The pressure change of CO_2 fracturing fluid in reservoir fractures and the fracture initiation ability can also be analysed using Equation (1).

Furthermore, the relationship between the density of CO_2 fracturing fluid and the pressure and temperature within the fracture can be observed through Equations (2) and (3), while the relationship between fluid viscosity and pressure is demonstrated in Equation (4) [41].

$$\rho = A_0 + A_1 P + A_2 P^2 + A_3 P^3 + A_4 P^4, \tag{2}$$

$$A_i = b_{i0} + b_{i1} T + b_{i2} T^2 + b_{i3} T^3 + b_{i4} T^4, \tag{3}$$

$$\mu = C_0 + C_1 P + C_2 P^2 + C_3 P^3 + C_4 P^4, \tag{4}$$

where T is the reservoir temperature, K. Ai and Bii is the intermediate parameters of the calculation process.

The stress field of the reservoir rock also exerts an influence on the seepage capacity of the CO_2 fracturing fluid, as demonstrated by Equations (5) and (6). In addition, the coupling relationship between the stress field and seepage field is reflected in the change in rock permeability caused by pore deformation.

$$\varphi = (\varphi_0 - \varphi_r) \exp(-\alpha_\varphi \sigma_{av}) + \varphi_r, \tag{5}$$

$$\sigma_p = (\alpha_1 + \alpha_2 + \alpha_3) \Big/ 3 - \alpha p, \tag{6}$$

in which φ_0 is the stress-free porosity. φ_r is the residual porosity. α_φ is the stress sensitivity coefficient of porosity. σ_p is the mean effective stress, MPa. σ_1, σ_2, and σ_3 are the principal stresses in all directions, MPa.

2.2. CO_2 Fluid Flow Model of Cohesive Pore Pressure Cell

CO_2 fracturing fluid in reservoir fractures behaves as a non-Newtonian fluid, and the most common fluidity observed in CO_2 fracturing fluid in reservoir fractures is characterised by two distinct flow patterns: tangential flow and normal flow (Figure 1). The tangential flow of the CO_2 fracturing fluid within the unit is aligned with the cohesive unit, whereas the normal flow is oriented perpendicularly to the upper and lower surfaces of the cohesive unit.

The tangential flow of the fracturing fluid is calculated in accordance with the Newtonian fluid flow equation (Equation (7)) [42].

$$q = \frac{w^2}{12\mu} \nabla p, \tag{7}$$

in which q is the density vector of CO_2 fracturing fluid, m/s. w presents a crack opening width, m.

The volume flow rate of the normal flow of CO_2 fracturing fluid on the upper and lower surfaces of the fracture extension unit can be calculated using Equation (8).

$$\begin{aligned} q_t &= c_t (p_i - p_t) \\ q_b &= c_b (p_i - p_b) \end{aligned} \tag{8}$$

in which q_t and q_b are considered as the volume flow rate of CO_2 fracturing fluid on the upper and lower surfaces of the fracture extension unit, m^3/s. In addition, c_t and c_b are

considered as the filtration coefficient on both sides of the crack, $m^3/(Pa \cdot s)$. p_t and p_b present the pore pressure on both sides of the fracture, MPa.

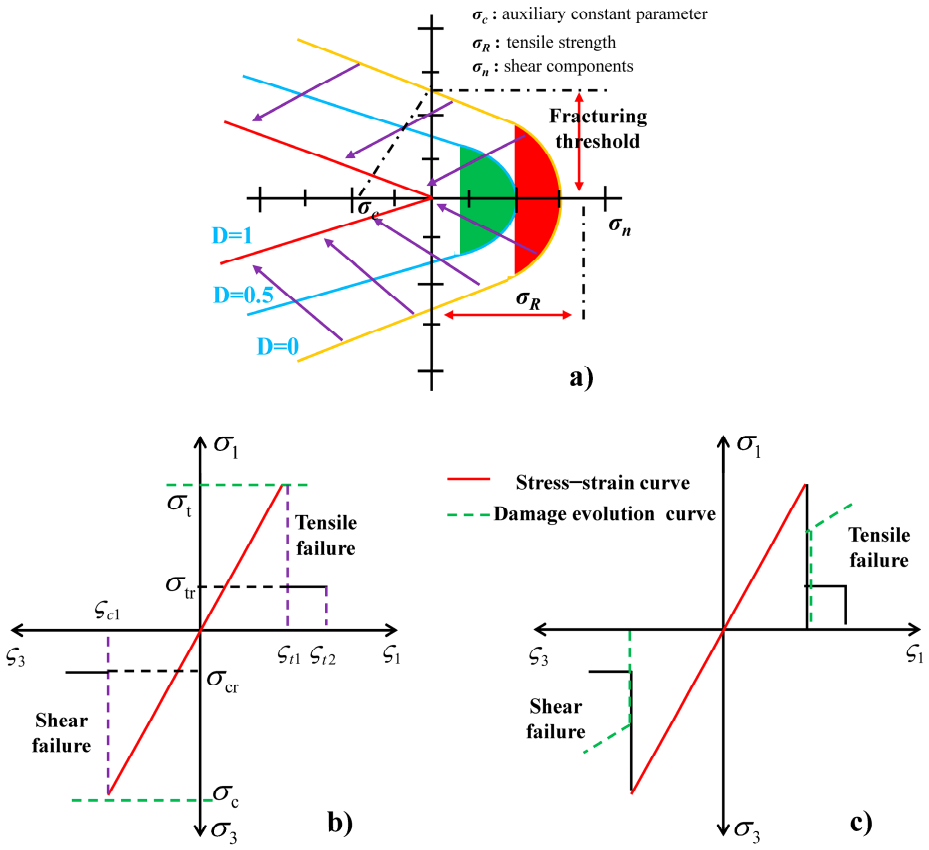

Figure 1. Cohesive unit damage model and simplified rock constitutive model. (**a**): Evolution of hyperbolic surfaces with damage plasticity criterion. (**b**): Elastic-brittle damage theory model. (**c**): Damage evolution model.

Simultaneously, the mass of CO_2 fluid inside the reservoir fracture can be calculated and analysed using Equation (9):

$$\nabla q - \frac{\partial w}{\partial t} + q_t + q_b = 0 \tag{9}$$

2.3. Crack Propagation Criterion Based on Damage Mechanics

The stress state satisfies the maximum tensile stress criterion, also known as the Mohr -Coulomb criterion, thereby achieving the maximum value required for damage to reservoir rock. Reservoir fractures can induce rock damage and facilitate crack propagation under the pressure exerted by CO_2 fracturing fluid.

The tensile failure criterion of reservoir rock fractures is shown in Equation (10), while the shear failure criterion can be calculated using Equation (11).

$$-\sigma_1 \geq \sigma_t, \tag{10}$$

where σ_t is the uniaxial tensile strength of the reservoir rock, and σ_1 is considered the maximum value required for reservoir rock to be damaged, MPa.

$$\sigma_1 - \sigma_3 \frac{1 + \sin\theta}{1 - \sin\theta} \geq f_c, \tag{11}$$

in which σ_3 is considered the minimum principal stress of reservoir rock, MPa. θ presents the internal friction angle, °. f_c is the uniaxial compressive strength of reservoir rock, MPa.

Furthermore, the damage variable D is introduced for the purpose of quantitative analysis of the damage degree of rock medium materials, and the isotropic of reservoir materials was demonstrated during rock damage. The value $D = 0$ indicates that the local unit of the rock model has not experienced any damage or crack propagation. However, a value of $D = 1$ signifies that the unit has sustained damage that may potentially result in a loss of bearing capacity.

The relationship between rock damage variables and strain during shear failure is described by Equation (12), while Equation (13) can be demonstrated to be the corresponding function for these variables during tensile failure.

$$\begin{array}{ll} D = 0, & \varsigma_{c1} < \varsigma \\ D = 1 + \frac{\sigma_{\mathrm{cr}}}{\varsigma E_0}, & \varsigma \le \varsigma_{c1} \end{array}, \tag{12}$$

$$\begin{array}{ll} D = 0, & \varsigma < \varsigma_{t1} \\ D = 1 - \frac{\sigma_{\mathrm{tr}}}{\varsigma E_0}, & \varsigma_{t1} < \varsigma \le \varsigma_{t2} \\ D = 1, & \varsigma_{t2} \le \varsigma \end{array}, \tag{13}$$

where ς_{t1} is the ultimate elastic tensile strain of rock, ς_{t2} presents an ultimate tensile strain of reservoir rock. ς_{c1} is considered as the compressive strain in ultimate elastic tension. σ_{tr} demonstrates the residual tensile strength of reservoir rocks, and σ_{cr} is the uniaxial residual compressive strength of a reservoir rock.

The fracture pressure of the reservoir rock can be expressed by Equation (14).

$$P_f = 3\sigma_{\mathrm{h}} - \sigma_{\mathrm{H}} - \alpha P_P + S_t \tag{14}$$

In which P_f is the fracture pressure of the reservoir rock, MPa. σ_{h} is the minimum horizontal ground stress, MPa. σ_{H} is the maximum horizontal ground stress, MPa. S_t is the tensile strength, MPa. P_P is a rock pore pressure, MPa. α is the effective stress coefficient.

In addition to the crack extension criteria mentioned in this study, other constitutive models that can be used to determine crack extension include stress intensity factor model, energy release rate model, plastic fracture mechanics model, continuum mechanics model, interface crack extension model, and fracture mechanics finite element model.

2.4. CO_2 Fracturing Model of Unconventional Low Permeability Reservoir Fractures

A cohesive unit damage model based on extended finite elements was developed to simulate the fracture propagation behaviour of CO_2 fracturing fluid in unconventional low-permeability shale reservoirs. A two-dimensional reservoir fracturing mesh model comprising 20,000 units was constructed to investigate the CO_2 fracturing process of directional perforation reservoirs, which is of considerable importance for the exploitation of unconventional reservoirs. Furthermore, mesh refinement was conducted in the vicinity of the wellbore with the objective of enhancing the convergence and precision of the model during operation. This approach proved effective in ensuring stability of the CO_2 fracturing process (Figure 2).

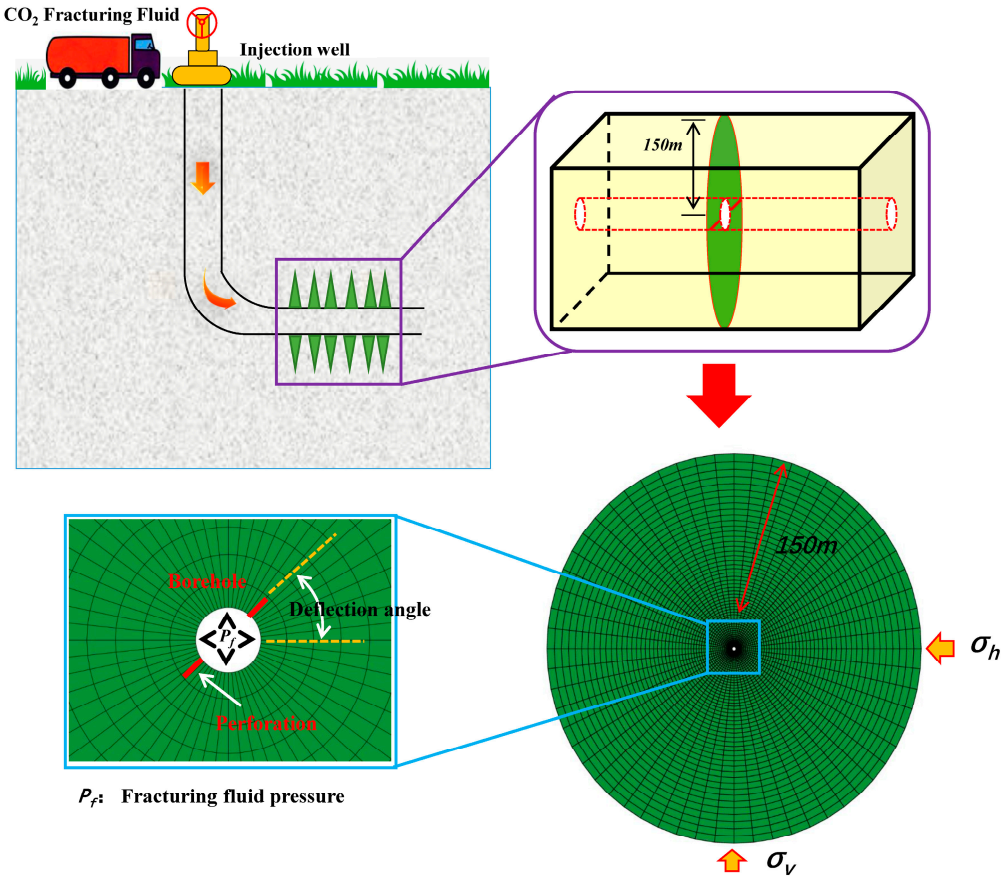

Figure 2. Finite element model of CO_2 fracturing in perforated horizontal wells in low permeability reservoirs.

Table 1 presents the pertinent parameters and data configuration employed to simulate the fracture expansion of low permeability reservoirs by CO_2 fracturing fluid.

Table 1. The characteristic parameters and the initial conditions of geological formations.

Parameter	Value	Parameter	Value
Elastic Modulus, E/GPa	25–35	Poisson's ratio, ν	0.24
Minimum horizontal principal stress, σ_h/MPa	32	Maximum horizontal principal stress, σ_H/MPa	37
Tensile strength, C/MPa	6	Initial pore pressure, Pip/MPa	20
Initial porosity, ϕ/%	8	Permeability, $\times 10^{-16}$ K/m^2	5–15
Leak-off coefficient	2.5×10^{-12}	Total fracturing time, T/min	15

3. Results and Discussion

3.1. Influence of Physical and Chemical Parameters of CO_2 Fracturing Fluid on the Crack Extension

The physical and chemical properties of CO_2 fracturing fluid, similar to those of water-based fracturing fluids, can significantly influence reservoir transformation and fracture propagation behaviour. The viscosity and rheological properties of CO_2 fracturing fluid are critical factors that contribute to variations in the propagation of fractures within the reservoir [43,44]. Previous studies have analysed and revealed the effect of water-based fracturing fluid viscosity (calculated using Equation (15)) on the expansion behaviour of low-permeability reservoir cracks and rock damage rules [45]. However, current research only focuses on the performance evaluation of CO_2 fracturing fluid, including aspects

such as fluid viscosity improvement and reservoir damage. Currently, the changing trend between the rheological parameters of CO_2 fracturing fluid and crack expansion has not been discussed in detail. The relationship curves between different thickener contents and the above two factors are shown in Figure 3.

$$\eta = \frac{\tau_w}{\gamma_w} = \frac{\Delta p D^2}{32 L v} \quad . \tag{15}$$

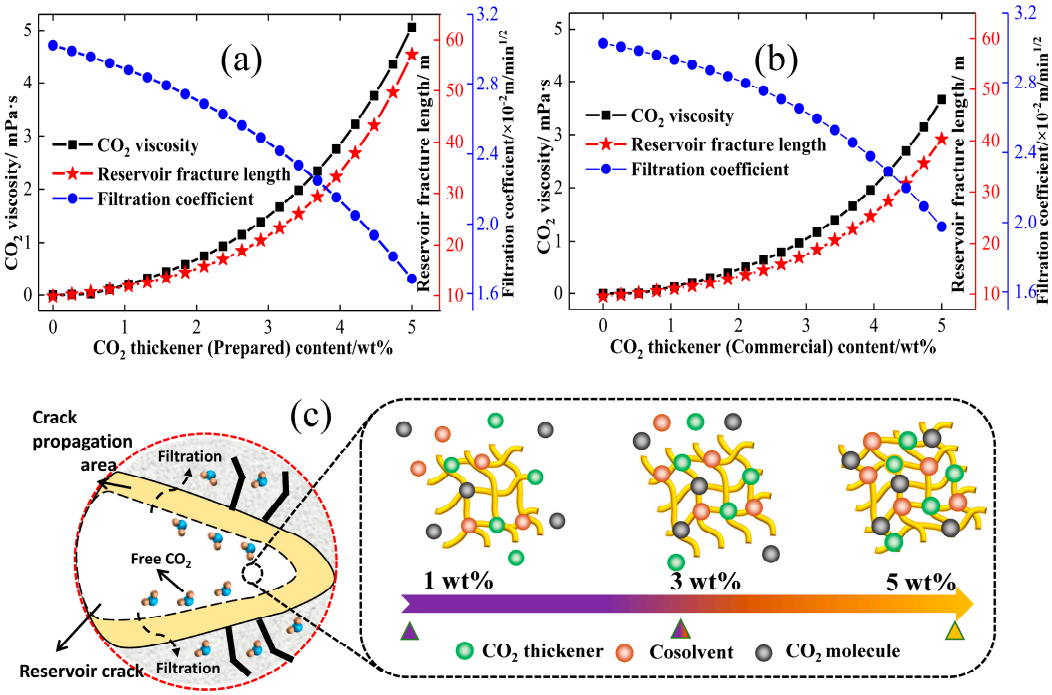

Figure 3. Effects of physical properties of CO_2 fracturing fluid on fluid viscosity, filtration coefficient and fracture propagation. (**a**): Effect of prepared CO_2 thickener. (**b**): Effect of commercial CO_2 thickener. (**c**): The morphology of each molecule in CO_2 fracturing fluid at different contents.

As shown in Figure 3, the addition of CO_2 thickener not only effectively enhances the rheological parameters (apparent viscosity) of CO_2 fracturing fluid, but also demonstrates an increase in both the crack extension length and the pressure within the reservoir crack. The extremely low viscosity of pure CO_2 fracturing fluid (0 wt%) is not conducive to the rapid initiation of damage to reservoir rock and crack formation. The low crack length and width of the fracturing fluid (0.02 mPa·s) is indicative of the low viscosity of the pure CO_2 fracturing fluid (0 wt%), which may be related to the fluid pressure in the reservoir fractures under low viscosity. The CO_2 fluid pressure in the reservoir fracture, as illustrated in Equation (7), is predominantly influenced by the viscosity of the injected fluid and the injection rate, and the injection rate is constant in the fracturing operation of a particular reservoir. Thus, the CO_2 fracturing fluid within the reservoir fractures has become the primary factor influencing fracture fluid pressure, directly determining whether the pressure within the fractures can exceed the minimum fracturing pressure required for reservoir stimulation. Additionally, the apparent viscosity of CO_2 fracturing fluid, at a constant flow rate as indicated in Equation (7), exhibits a significant positive correlation with the fluid pressure within the reservoir fractures, thereby offering valuable insight for enhancing the fracture propagation of CO_2 fracturing fluid. The exceptionally low viscosity of pure CO_2 fracturing fluid (Figure 3) results in a low intra-fracture pressure that is insufficient to overcome the minimum fracturing pressure of the reservoir, thereby

resulting in a diminished fracture propagation behaviour under conditions of extremely low viscosity [46].

As demonstrated in Figure 3, the low CO_2 thickener content results in a negligible increase in the apparent viscosity of CO_2 fracturing fluid. Furthermore, the crack extension length demonstrates a strong positive correlation with the apparent viscosity. When the CO_2 thickener concentration is increased to 3 wt%, the fracture propagation ability exhibits a pronounced exponential growth trend, accompanied by a significant increase in the apparent viscosity of the CO_2 fracturing fluid. The pressure exerted by CO_2 fracturing fluid on reservoir fractures can exceed the minimum fracture initiation pressure of rocks, thereby becoming a significant factor in the fracture expansion behaviour. However, the underlying reason for the observed differences in expansion capabilities is attributed to the CO_2 viscosity μ, which is directly associated with the fluid pressure within the reservoir fractures.

The relationship between the apparent viscosity of CO_2 fracturing fluid and the crack extension can be analysed using the micro-grid model of CO_2 fracturing fluid. Pure CO_2 fracturing fluid exhibits a lack of intermolecular interactions and intermolecular forces, resulting in a weak apparent viscosity and crack extension length. Furthermore, the large filtration volume formed by pure CO_2 fracturing fluid contributes to the reduction in crack length growth. The addition of a CO_2 thickener has been shown to increase the intermolecular bonds between CO_2, co-solvent, and thickener, thereby facilitating the micro-grid density of CO_2 fracturing fluid [47]. The enhanced micro-grid density is evident not only in the apparent viscosity of CO_2 fracturing fluid, but also in the reduction in filtration volume due to the mutual entanglement of molecules [48]. The drag effect of other molecules hinders the penetration of a large number of microscopic molecules into the reservoir through the pores of the fracture. Consequently, the CO_2 fluid in the fracture can be rapidly compressed to the minimum fracturing pressure of the reservoir in a shorter time. CO_2 fracturing fluid with higher viscosity promotes the formation of larger intermolecular bonds and denser microscopic networks with other molecules compared to low-viscosity fluids. As a result, nearly all CO_2 fracturing fluid remains within the reservoir fractures, where it exerts pressure to facilitate rapid fracture expansion.

Moreover, this study elected to utilise a commercial CO_2 thickener as a control, with the objective of analysing the fracture propagation behaviour of CO_2 fracturing fluid on low permeability reservoirs under different thickeners. The experimental results presented in Figure 3 demonstrate that commercially available thickeners, irrespective of their thickener content, exhibit a comparatively diminished capacity for CO_2 thickening and crack extension in comparison to the prepared thickeners. This observation may be attributed to the micro-grid density and interaction bonds resulting from the molecular structure disparities between the two thickeners. The side chains of synthetic thickeners contain a large number of CO_2-philic groups, which enable CO_2 molecules to establish closer intermolecular attraction and intermolecular chemical bonds with synthetic thickeners. Additionally, the microscopic grid of the fracturing fluid hinders the escape of CO_2, thereby facilitating its effective filtration and subsequent pressure buildup within the fissures of the rock matrix. This phenomenon contributes to the expeditious initiation and progression of the fracturing process, leading to the effective fragmentation of the target rock fracture. However, the absence of CO_2-philic groups in commercial thickener molecules has been demonstrated to weaken the formation of intermolecular chemical bonds and microscopic grids with thickeners and cosolvents. Furthermore, a substantial quantity of free CO_2 molecules has been observed to be present in CO_2 fracturing fluids. Free CO_2 molecules that are not bound by commercial thickeners can easily filter into reservoir rocks and reduce the fluid pressure in the fractures. The CO_2 fluid in the fractures, which cannot meet the minimum

fracturing pressure of the reservoir, naturally forms a smaller fracture expansion behaviour. Therefore, the rheological parameters (apparent viscosity) of CO_2 fracturing fluid serve as a critical factor influencing the expansion of reservoir fractures, with a strong positive correlation observed between apparent viscosity and fracture length. The incorporation of CO_2 thickener significantly enhances both the apparent viscosity of CO_2 and the ability to expand fractures.

3.2. Effects of Reservoir Permeability and Elastic Modulus on the Crack Extension

As mentioned in Figure 3, the filtration capacity of the CO_2 fracturing fluid at the edge of reservoir fractures exerts a direct influence on the expansion capacity of the CO_2 fracturing fluid to reservoir fractures. Furthermore, the permeability of reservoir rock constitutes a significant geological parameter, which in turn impacts the fluid filtration coefficient (Figure 4). Figure 4a,b illustrated the variations in the filtration coefficient and fracture length of CO_2 fracturing fluid under different reservoir permeabilities. reservoir fractures in low-permeability reservoirs exhibit accelerated fracture expansion capabilities, while the filtration capacity of the CO_2 fracturing fluid is notably enhanced due to the reduced reservoir permeability. The capacity of CO_2 fracturing fluid to achieve optimal fracture expansion behaviour under conditions of low permeability can be attributed to the diminished filtration coefficient that is characteristic of such conditions. The CO_2 fracturing fluid in the reservoir fracture will contact the fracture surface in both normal and tangential directions, and the permeability of the fracture surface directly determines whether the CO_2 molecules in the CO_2 fracturing fluid can easily enter the rock through the rock pores to achieve fluid filtration behaviour. CO_2 fracturing fluid encounters fewer surface pores on the fractures of low-permeability reservoirs, which significantly reduces fluid filtration. As a result, a substantial volume of CO_2 fracturing fluid can be gradually compressed within the reservoir fractures, reaching the minimum fracture initiation pressure of the reservoir rock, thereby inducing relatively rapid and intense fracture expansion in low-permeability reservoirs.

An increase in reservoir permeability significantly reduces the fracture expansion capacity, and the length of the fractures exhibits a marked decrease under conditions of high permeability in reservoir rocks [49]. The relationship between reservoir permeability and fracture expansion capacity is strongly inverse, while the filtration coefficient of CO_2 fracturing fluid shows a clear positive correlation with reservoir permeability. Consequently, a higher filtration coefficient of CO_2 fracturing fluid is observed in reservoir rocks with greater permeability, which presents a significant challenge to the ability of CO_2 fracturing fluid to achieve the minimum fracturing pressure in the reservoir fractures. Numerous CO_2 fracturing fluids will infiltrate the larger pores of the reservoir on the rock surface at the edge of the crack, thereby substantially diminishing the volume of CO_2 fracturing fluid remaining in the reservoir cracks. The internal pressure within the fractures cannot be effectively maintained at the minimum fracture initiation pressure due to the filtration of a considerable amount of CO_2 fracturing fluid, thereby weakening the fracture expansion behaviour in high permeability reservoirs [50].

Simultaneously, the elastic modulus of the reservoir rock demonstrates a comparable growth trend to the reservoir permeability, and the elastic modulus and the fracture length exhibit a highly precise positive proportional relationship. The correlation between the elastic modulus and the reservoir fracture expansion capacity can be ascribed to the filtration capacity of the fracture surface under varying elastic moduli, which directly determines the degree of force exerted on the fracture tip by the CO_2 fracturing fluid. The low elastic modulus of the rock will cause significant damage to the surface pores in the vicinity of the reservoir fractures. Furthermore, a low fluid pressure can cause

the surface pores to be squeezed and expanded [51]. The ingress of CO_2 fracturing fluid into the rock is facilitated by the ever-increasing surface pores and microcracks, thereby directly increasing the filtration volume of the fracturing fluid in the reservoir fractures. The larger filtration volume under low elastic modulus will reduce the fluid pressure in the reservoir fractures, resulting in a smaller fracture expansion capacity. However, the surface of reservoir fractures with a high elastic modulus demonstrates greater material strength, which hinders the ability of CO_2 fracturing fluid to open surface pores and infiltrate the rock. In contrast, a significant volume of CO_2 fracturing fluid will concentrate at the shear zone of the fractures, increasing the applied force at the fracture tip, thereby facilitating rapid rock damage and fracture propagation at the fracture tip.

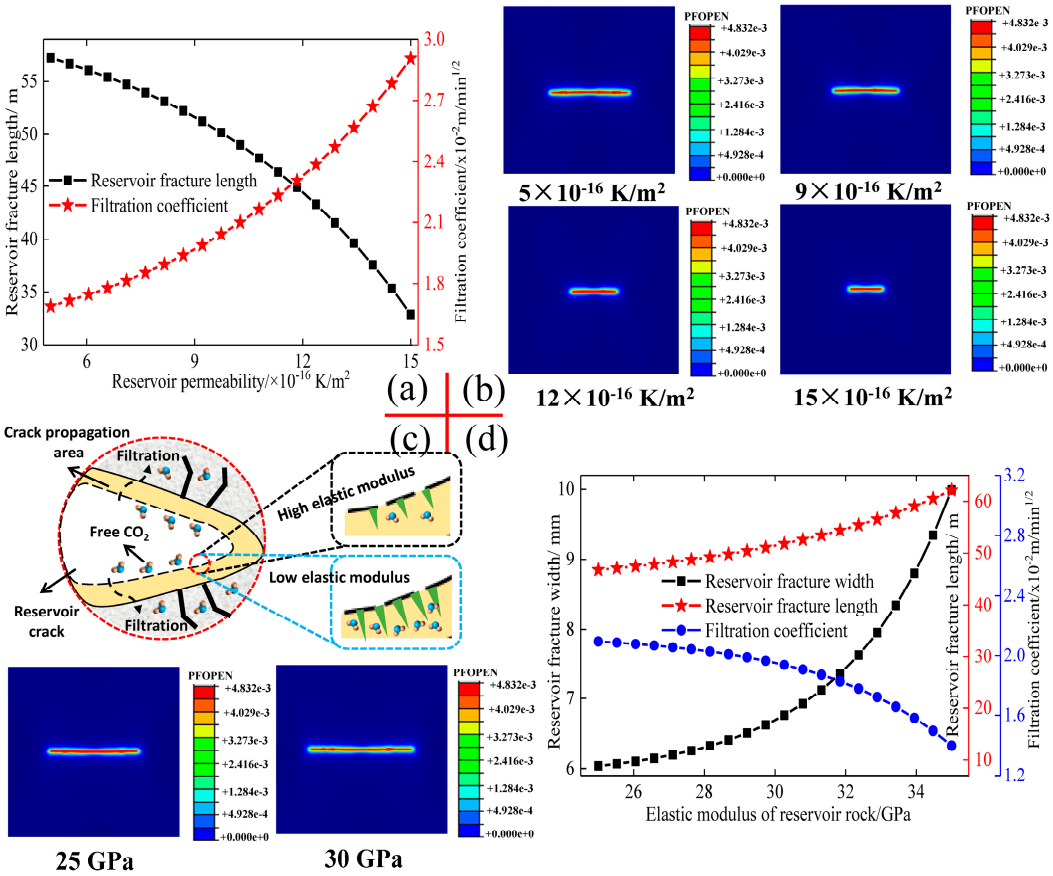

Figure 4. Effects of reservoir permeability and elastic modulus on fluid filtration coefficient and fracture propagation. (**a**): Effect of reservoir permeability. (**b**): Effect of reservoir permeability on the crack morphology. (**c**): Effect of elastic modulus on the crack morphology. (**d**): Effect of elastic modulus.

3.3. Effects of Reservoir Temperature on the Crack Extension

Reservoir temperature, as a key performance indicator of CO_2 fracturing fluid, is frequently utilised to examine the significant impact of CO_2 fracturing fluid on the expansion of reservoir fractures. To assess the reservoir applicability of CO_2 fracturing fluid, this study investigates the fracture extension behaviour induced by CO_2 fracturing fluid at various reservoir temperatures [52]. The reservoir temperatures depicted in Figure 5 are derived from the analysis of common shale reservoirs situated at an approximate depth of 3000 m, as the temperature increases by 25 °C to 30 °C per kilometre of depth. Figure 5 illustrates the changing trends of fracture expansion parameters and the filtration coefficient of CO_2 fracturing fluid at varying reservoir temperatures, thereby offering a valuable reference point for investigating the expansion laws and enhancement measures of reservoir fractures

in the diverse geological factors. As demonstrated in Figure 5, the reservoir temperature not only exerts a substantial influence on the capacity of CO_2 fracturing fluid to expand within reservoir fractures, but also has a significant change in the properties of CO_2 fracturing fluid. The length of the reservoir fractures increases gradually with an increase in the reservoir temperature. The filtration volume of the CO_2 fracturing fluid in the reservoir fractures also shows a clear positive proportional relationship with the reservoir temperature. Furthermore, an examination of the curve changes in the extension length and fluid filtration in Figure 5 suggests the presence of a causal relationship between the aforementioned parameters. Simultaneously, the apparent viscosity of CO_2 fracturing fluid decreases rapidly with the increase in reservoir temperature, which may be a significant factor contributing to the reduction in the filtration volume of CO_2 fracturing fluid.

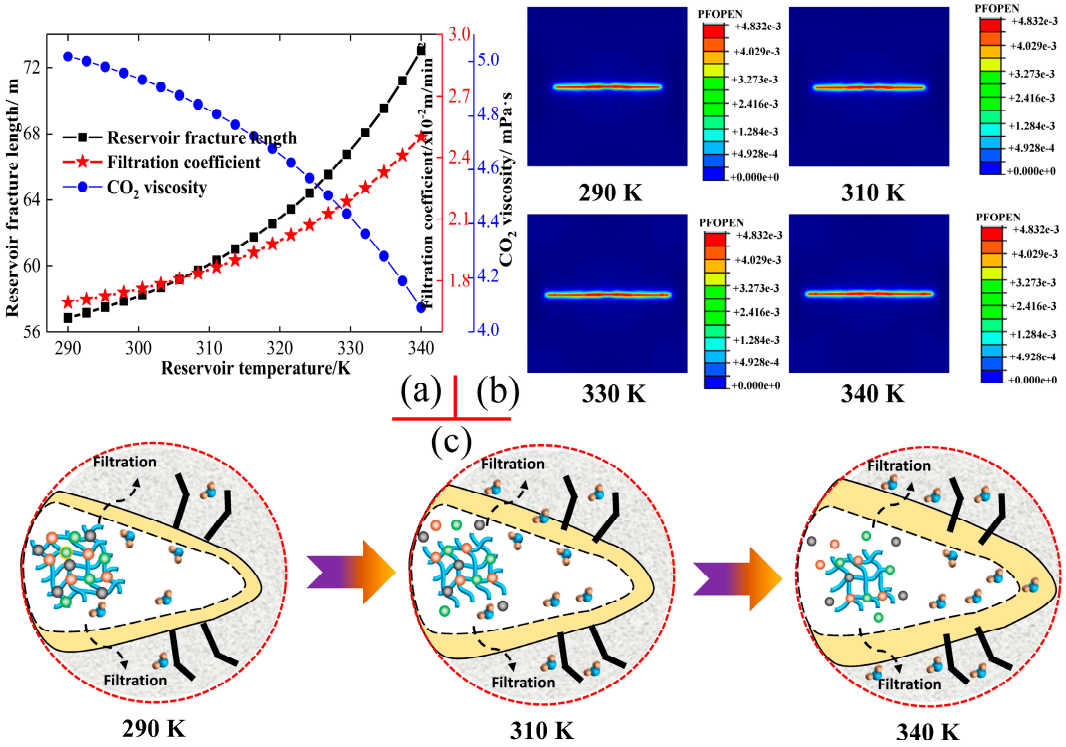

Figure 5. Effects of reservoir temperature on fluid filtration coefficient, fluid viscosity, and fracture propagation. (**a**): Effect of reservoir temperature. (**b**,**c**): Changing in the crack morphology.

The molecular activity of CO_2 fracturing fluid in reservoir fractures is influenced by reservoir temperature, which serves as a microscopic factor driving fracture expansion in unconventional reservoirs. The Arrhenius equation [53] effectively describes the impact of reservoir temperature on the molecular motion and the subsequent changes in fracture expansion behaviour. The molecules connected by chemical bonds in the reservoir fractures are unable to break free due to the reduced molecular activity at low reservoir temperature, which in turn reduces the molecules' ability to undergo irregular Brownian motion. The chemical bonds within CO_2 fracturing fluid molecules also hinder the formation of free molecules, and the denser microscopic grid further reduces the filtration coefficient. Additionally, the smaller filtration coefficient experiences a reduction in effectiveness due to the denser microscopic grid. The extremely small CO_2 filtration can promote the continuous accumulation of CO_2 fracturing fluid in the reservoir fractures and hold the pressure to the minimum fracturing pressure. However, the apparent viscosity of the CO_2 fracturing fluid is still the biggest factor in the CO_2 holding pressure to the minimum fracturing pressure. The fluid pressure of CO_2 fracturing fluid with a constant flow rate in the reservoir

fractures, as described by Equation (7), exhibits a strong proportional relationship with the apparent viscosity of the CO_2 fluid. This directly results in higher fluid pressure for CO_2 with a high viscosity at low temperatures. However, an increase in reservoir temperature leads to a significant enhancement in the expansion capacity of reservoir fractures, although it concurrently results in a substantial reduction in the apparent viscosity of CO_2 fracturing fluid. Additionally, the volume of fluid loss progressively increases with rising reservoir temperature, which are salient factors contributing to the reduction in fracture expansion capacity. The significant enhancement of reservoir fracture expansion capacity at elevated temperatures is likely an inevitable consequence of the volumetric expansion of CO_2 fracturing fluid. The positive effect of this factor may overshadow the adverse impact caused by the reduction in apparent viscosity and the increase in filtration volume at high temperatures.

Whilst the activity of each molecule in the CO_2 fracturing fluid is significantly weakened at elevated temperatures, a substantial number of molecules connected by intermolecular chemical bonds are stretched and lengthened or broken due to the enhanced activity of high temperature [54,55]. The reduction in microscopic grid density and the breaking of chemical bonds directly lead to the weakening of macroscopic apparent viscosity [56]. The weakened fluid pressure, resulting from the apparent viscosity, hinders the effective expansion of reservoir fractures at elevated temperatures. Additionally, the dissociation of chemical bonds between molecules at elevated temperatures gives rise to a substantial number of free molecules within the CO_2 fracturing fluid. These molecules are able to penetrate the rock surface of reservoir fractures with greater efficiency and subsequently infiltrate the rock interior. The high loss volume at elevated temperatures is also detrimental to the pressure holding capacity of the CO_2 fracturing fluid within reservoir fractures, and the high loss volume factor will also reduce the impact on the expansion capacity of reservoir fractures. While elevated reservoir temperatures may indeed reduce fluid viscosity and increase fluid loss volume, this is not conducive to the fracture expansion behaviour of low-permeability reservoirs. Conversely, an increase in reservoir temperature will significantly augment the repulsive force between molecules in the CO_2 fracturing fluid, thereby facilitating the macroscopic expansion of fluid volume in reservoir fractures. As demonstrated in Figure 5, the volume expansion of CO_2 fracturing fluid due to elevated temperatures emerges as the pivotal factor in facilitating the sustained augmentation of reservoir fracture length. This is in contrast to the filtration and viscosity reduction of CO_2 fracturing fluid, which impede the growth rate of fracture extension.

3.4. Effects of Reservoir Pressure on the Crack Extension

As a distinct geological parameter, reservoir pressure has emerged as a crucial factor that significantly influences the performance of CO_2 fracturing fluid and fracture propagation. Variations in reservoir pressure play a pivotal role in determining the production efficiency and fracture development in low-permeability shale reservoirs [57]. As illustrated in Figure 6, the fracture propagation behaviour of low permeability shale reservoirs is observed under varying reservoir pressures, along with the alterations in numerous properties of CO_2 fracturing fluid within the fractures. A notable fracture length growth trend is evident, and the apparent viscosity of the CO_2 fracturing fluid undergoes a gradual increase with rising reservoir pressure. Conversely, the filtration coefficient of the CO_2 fracturing fluid exhibits a pronounced inverse proportional relationship with reservoir pressure [58]. Furthermore, as demonstrated in Figure 6, the impact of reservoir pressure on the expansion behaviour of reservoir cracks is predominantly attributable to alterations in the apparent viscosity and loss volume of the CO_2 fracturing fluid. The variations in the micro-grid and intermolecular bonds under the action of reservoir pressure directly govern

the initiation and expansion capabilities of reservoir cracks. Low reservoir pressure results in a relatively greater intermolecular distance in CO_2 fracturing fluid, as the reduced external pressure fails to compress the molecules [59]. Consequently, a significant proportion of CO_2 fracturing fluid molecules remain in a relatively free state due to the increased spacing, while those connected by intermolecular forces exhibit weaker bond energies and longer bond lengths [60,61]. The longer chemical bonds under low reservoir pressure results in a reduction in the microscopic grid density, which directly correlates with a decrease in fluid viscosity at the macroscopic level. The constant flow rate of CO_2 fracturing fluid, as described in Equation (7), also exhibits a significantly lower fracture pressure at reduced fluid viscosity [62], making it difficult to overcome the minimum fracture initiation pressure of the reservoir rock [63]. Additionally, free compound molecules that lack chemical bonds under low reservoir pressure can readily seep into the reservoir rock on the fracture surface, further exacerbating the challenge of reservoir fracture expansion.

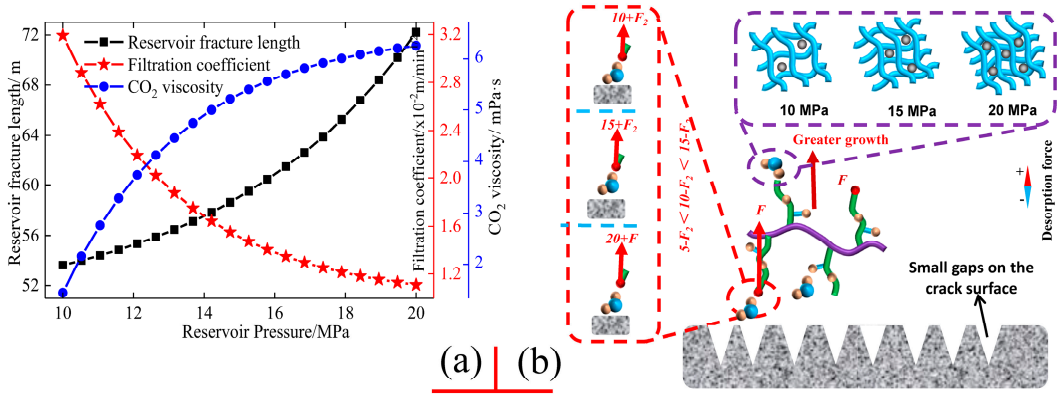

Figure 6. Effects of reservoir pressure on fluid filtration coefficient, fluid viscosity, and fracture propagation (**a**,**b**).

Immediately, the increase in reservoir pressure will not only gradually alter the expansion behaviour of the aforementioned reservoir fractures, but also significantly affect the fluid properties of the CO_2 fracturing fluid within the fractures, such as the apparent viscosity and filtration coefficient [64,65]. The increase in reservoir pressure will compress the CO_2 fracturing fluid within the reservoir fractures, reducing the distance between molecules at the microscopic level, thus resulting in a state not observed under low pressure [66,67]. Molecules connected by chemical bonds at greater distances will gradually move closer, shortening the bond lengths under low pressure [68]. The bond energy of these chemical bonds will also increase due to the compression induced by the elevated pressure. Additionally, free molecules that were previously unbonded under low pressure will begin to form chemical bonds under the influence of high-pressure compression, thereby enhancing the density of the microscopic grid of the CO_2 fracturing fluid [69]. This increased microscopic grid density leads to a higher macroscopic fluid viscosity, which in turn contributes to a rise in fluid pressure within the reservoir fractures, facilitating fracture expansion [70]. Concurrently, the formation of chemical bonds between free molecules will also contribute to a reduction in the filtration volume of CO_2 fracturing fluid, which has become an important component of enhancing the fluid pressure in reservoir fractures [71]. The decreased filtration volume implies that a greater volume of CO_2 fracturing fluid remains within the fractures, resulting in a more rapid increase in pressure, ultimately reaching the minimum fracture initiation pressure of the reservoir rock and facilitating fracture expansion. Thus, CO_2 fracturing fluid not only exhibits a reduced filtration coefficient in reservoir fractures under higher reservoir pressure, but also demonstrates increased fluid viscosity and enhanced fracture expansion capacity as a result of the elevated reservoir

pressure. Furthermore, the experimental findings presented in Figures 5 and 6 demonstrate that the CO_2 fracturing fluid developed in this study can meet the fracture expansion requirements of low-permeability reservoirs under conditions of high temperature and high pressure.

3.5. Impact on Industrial Carbon Dioxide Fracturing Fluid Technology

The utilisation of CO_2 fracturing technology in unconventional reservoirs or low permeability reservoirs is currently in its infancy due to numerous existing defects, including extremely low fluid viscosity, significant fluid loss and unclear fracture expansion rules. The fracture expansion rules of CO_2 fracturing fluid in unconventional reservoirs explored in this study have the potential to effectively guide the efficient exploitation of CO_2 fracturing technology in unconventional shale reservoirs. Furthermore, these rules can also guide the fracturing production increase evaluation at the oil field site. Moreover, the fracture expansion rules explored in this study can provide a practical and effective supplement to shale resources, thereby addressing the shortage of conventional energy.

4. Conclusions

This study developed a mathematical model for CO_2 fracturing crack expansion in unconventional low-permeability reservoirs based on the coupled seepage–stress–damage framework, which facilitates the exploration of the impact of various geological conditions and fluid factors on the fracture expansion behaviour. Additionally, the micro-grid model and molecular dynamics approach were employed to uncover the underlying mechanisms by which each factor influences the fluid characteristics of CO_2 fracturing fluid and crack expansion. The variations in the rheological and filtration parameters of CO_2 fracturing fluid within reservoir fractures are critical factors that directly influence fracture propagation behaviour. Meanwhile, the formation of chemical bonds between microscopic molecules and the density of the microscopic grid serve as the fundamental mechanisms driving fracture propagation. Furthermore, rock properties such as permeability or elastic modulus can achieve fracture expansion by altering the minimum fracture initiation pressure or the brittleness of rock damage. An increase in reservoir temperature and pressure can result in an augmentation of fracture length by 15 m and 19 m, respectively, and an escalation in reservoir permeability diminishes the fracture length by 21 m. Concurrently, the CO_2 fracturing fluid system constructed in this study also exhibits excellent fracture expansion ability in comparison to CO_2 fracturing fluid containing commercially available thickeners. This provides extensive scope for the application of CO_2 fracturing technology in unconventional low-permeability reservoirs. Concurrently, the practical implementation of CO_2 fracturing technology in numerous real oil fields has corroborated the observed trend of crack expansion in this study.

Author Contributions: Conceptualization, Q.L. (Qiang Li), Q.L. (Qingchao Li) and F.W.; methodology, H.C. and F.W.; validation, Y.W. and J.W.; formal analysis, Q.L. (Qiang Li) and Q.L. (Qingchao Li). All authors have read and agreed to the published version of the manuscript.

Funding: This research sponsored by Henan Provincial Science and Technology Research Project (242102320342), the Fundamental Research Funds for the Universities of Henan Province (NSFRF240616).

Data Availability Statement: The original contributions presented in this study are included in the article. Further inquiries can be directed to the corresponding authors.

Conflicts of Interest: The authors declare no conflicts of interest.

References

1. Wanniarachchi, W.A.M.; Ranjith, P.G.; Perera, M.S.A. Shale gas fracturing using foam-based fracturing fluid: A review. *Environ. Earth Sci.* **2017**, *76*, 91. [CrossRef]
2. Li, Q.; Li, Y.; Cheng, Y.; Li, Q.; Wang, F.; Wei, J.; Ansari, U. Numerical simulation of fracture reorientation during hydraulic fracturing in perforated horizontal well in shale reservoirs. *Energy Sources Part A Recovery Util. Environ. Eff.* **2018**, *40*, 1807–1813. [CrossRef]
3. Lv, Q.; Li, Z.; Li, B.; Zhang, C.; Shi, D.; Zheng, C.; Zhou, T. Experimental study on the dynamic filtration control performance of N_2/liquid CO_2 foam in porous media. *Fuel* **2017**, *202*, 435–445. [CrossRef]
4. Liu, Y.F.; Zhou, L.; Wan, X.C.; Tang, Y.F.; Liu, Q.; Li, W.; Liao, J.B. Synthesis and characterization of a temperature sensitive microcapsule gelling agent for high-temperature acid release. *ACS Omega* **2024**, *9*, 20849–20858. [CrossRef]
5. Hu, J.; Tang, Q.; Wu, Z.; Zhang, B.; He, C.; Chen, Q. Optimization and assessment method for total energy system retrofit in the petrochemical industry considering clean energy substitution for fossil fuel. *Energy Convers. Manag.* **2023**, *284*, 116967. [CrossRef]
6. Zou, C.; Xiong, B.; Xue, H.; Zheng, D.; Ge, Z.; Wang, Y.; Jiang, L.; Pan, S.; Wu, S. The role of new energy in carbon neutral. *Pet. Explor. Dev.* **2021**, *48*, 480–491. [CrossRef]
7. Li, Q.; Liu, J.; Wang, S.; Guo, Y.; Han, X.; Li, Q.; Cheng, Y.; Dong, Z.; Li, X.; Zhang, X. Numerical insights into factors affecting collapse behavior of horizontal wellbore in clayey silt hydrate-bearing sediments and the accompanying control strategy. *Ocean Eng.* **2024**, *297*, 117029. [CrossRef]
8. Abdelaal, A.; Aljawad, M.S.; Alyousef, Z.; Almajid, M.M. A review of foam-based fracturing fluids applications: From lab studies to field implementations. *J. Nat. Gas Sci. Eng.* **2021**, *95*, 104236. [CrossRef]
9. Was, G.S.; Petti, D.; Ukai, S.; Zinkle, S. Materials for future nuclear energy systems. *J. Nucl. Mater.* **2019**, *527*, 151837. [CrossRef]
10. Chen, X.; Qiu, R.; Wu, X. Multi-timescale capacity configuration optimization of energy storage equipment in power plant-carbon capture system. *Appl. Therm. Eng.* **2023**, *227*, 120371. [CrossRef]
11. Zhang, W.; Wan, L.; Fan, Y.; Zhang, X.; Zhou, J.; Chen, Y.; Li, H.; Liu, X.; Zhang, Y.; Wang, L. Construction and mechanism study of clean N_2 foam fracturing fluid stabilized by viscoelastic surfactant in concentrated brines for unconventional oil and gas. *J. Mol. Liq.* **2023**, *390*, 123168. [CrossRef]
12. Li, Q.; Li, Q.; Han, Y. Numerical Investigation on Kick Control with Displacement Kill Method during Well Test in Deep-water Gas Reservoir: Case Study. *Processes* **2024**, *12*, 2090. [CrossRef]
13. Zhang, H.; Yang, H.; Sarsenbekuly, B.; Zhang, M.; Jiang, H.; Kang, W.; Aidarova, S. The advances of organic chromium based polymer gels and their application in improved oil recovery. *Adv. Colloid Interface Sci.* **2020**, *282*, 102214. [CrossRef] [PubMed]
14. Li, H.; Shi, Y. Study on the performance degradation of sandstone under acidification. *ACS Omega* **2020**, *5*, 28333–28340. [CrossRef] [PubMed]
15. Zhang, F.; Wang, X.; Tang, M.; Du, X.; Xu, C.; Tang, J.; Damjanac, B. Numerical investigation on hydraulic fracturing of extreme limited entry perforating in plug-and-perforation completion of shale oil reservoir in Changqing oilfield, China. *Rock Mech. Rock Eng.* **2021**, *54*, 2925–2941. [CrossRef]
16. Zhong, X.; Chen, J.; An, R.; Li, K.; Chen, M. A state-of-the-art review of nanoparticle applications with a focus on heavy oil viscosity reduction. *J. Mol. Liq.* **2021**, *344*, 117845. [CrossRef]
17. Chen, X.; Wang, N.; Xia, S. Research progress and development trend of heavy oil emulsifying viscosity reducer: A review. *Pet. Sci. Technol.* **2021**, *39*, 550–563. [CrossRef]
18. Akpan, E.U.; Enyi, G.C.; Nasr, G.; Yahaya, A.A.; Ahmadu, A.A.; Saidu, B. Water-based drilling fluids for high-temperature applications and water-sensitive and dispersible shale formations. *J. Pet. Sci. Eng.* **2019**, *175*, 1028–1038. [CrossRef]
19. Huang, R.; Lei, Q.; Chen, J.; Weng, D.; Wang, X.; Liang, H. Gas content prediction model of water-sensitive shale based on gas–water miscible competitive adsorption. *Pet. Sci. Technol.* **2024**, *42*, 1841–1863. [CrossRef]
20. Li, M.; Liang, J.; Dou, Y. Experimental Study on Mechanical Properties of Rock in Water-Sensitive Oil and Gas Reservoirs Under High Confining Pressure. *Appl. Sci.* **2024**, *14*, 11478. [CrossRef]
21. Liew, M.S.; Danyaro, K.U.; Zawawi, N.A.W.A. A comprehensive guide to different fracturing technologies: A review. *Energies* **2020**, *13*, 3326. [CrossRef]
22. Montgomery, C.T.; Smith, M.B. Hydraulic fracturing: History of an enduring technology. *J. Pet. Technol.* **2010**, *62*, 26–40. [CrossRef]
23. Lei, Q.; Xu, Y.; Cai, B.; Guan, B.; Wang, X.; Bi, G.; Li, H.; Li, S.; Ding, B.; Fu, H.; et al. Progress and prospects of horizontal well fracturing technology for shale oil and gas reservoirs. *Pet. Explor. Dev.* **2022**, *49*, 191–199. [CrossRef]
24. Wang, J.; Elsworth, D.; Wu, Y.; Liu, J.; Zhu, W.; Liu, Y. The influence of fracturing fluids on fracturing processes: A comparison between water, oil and SC-CO_2. *Rock Mech. Rock Eng.* **2018**, *51*, 299–313. [CrossRef]
25. Wanniarachchi, W.A.M.; Ranjith, P.G.; Perera, M.S.A.; Rathnaweera, T.D.; Zhang, D.C.; Zhang, C. Investigation of effects of fracturing fluid on hydraulic fracturing and fracture permeability of reservoir rocks: An experimental study using water and foam fracturing. *Eng. Fract. Mech.* **2018**, *194*, 117–135. [CrossRef]

26. Li, N.; Yu, J.; Wang, C.; Zhang, S.; Liu, X.; Kang, J.; Wang, Y.; Dai, Y. Fracturing technology with carbon dioxide: A review. *J. Pet. Sci. Eng.* **2021**, *205*, 108793.
27. Middleton, R.; Viswanathan, H.; Currier, R.; Gupta, R. CO_2 as a fracturing fluid: Potential for commercial-scale shale gas production and CO_2 sequestration. *Energy Procedia* **2014**, *63*, 7780–7784. [CrossRef]
28. Huang, Q.; Liu, S.; Wang, G.; Cheng, W. Evaluating the changes of sorption and diffusion behaviors of Illinois coal with various water-based fracturing fluid treatments. *Fuel* **2021**, *283*, 118884. [CrossRef]
29. Li, Q.; Zhao, D.; Yin, J.; Zhou, X.; Li, Y.; Chi, P.; Han, Y.; Ansari, U.; Cheng, Y. Sediment instability caused by gas production from hydrate-bearing sediment in Northern South China Sea by horizontal wellbore: Evolution and mechanism. *Nat. Resour. Res.* **2023**, *32*, 1595–1620. [CrossRef]
30. Gu, M.; Mohanty, K.K. Rheology of polymer-free foam fracturing fluids. *J. Pet. Sci. Eng.* **2015**, *134*, 87–96. [CrossRef]
31. Wamock, W.E., Jr.; Harris, P.C.; King, D.S. Successful field applications of CO_2-foam fracturing fluids in the Arkansas-Louisiana-Texas region. *J. Pet. Technol.* **1985**, *37*, 80–88. [CrossRef]
32. Harris, P.C.; Reidenbach, V.G. High-temperature rheological study of foam fracturing fluids. *J. Pet. Technol.* **1987**, *39*, 613–619. [CrossRef]
33. Li, S.; Wang, Q.; Zhang, K.; Li, Z. Monitoring of CO_2 and CO_2 oil-based foam flooding processes in fractured low-permeability cores using nuclear magnetic resonance (NMR). *Fuel* **2020**, *263*, 116648. [CrossRef]
34. Li, Q.; Cheng, Y.; Li, Q.; Ansari, U.; Liu, Y.; Yan, C.; Lei, C. Development and verification of the comprehensive model for physical properties of hydrate sediment. *Arab. J. Geosci.* **2018**, *11*, 325. [CrossRef]
35. Shaikh, A.; Dai, C.; Sun, Y.; You, Q.; Qureshi, A.S.; Zhao, G.; Foutou, V.; Bakhsh, A.; Khan, N.; Abro, Z.; et al. Performance evaluation of a novel CO_2-induced clean fracturing fluid in low permeability formations. *J. Pet. Sci. Eng.* **2022**, *208*, 109674. [CrossRef]
36. Sinal, M.L.; Lancaster, G. Liquid CO_2 fracturing: Advantages and limitations. *J. Can. Pet. Technol.* **1987**, *26*. [CrossRef]
37. Zhao, J.; Wu, T.; Pu, W.; Du, D.; Chen, Q.; Chen, B.; Li, J.; Huang, Y. Application status and research progress of CO_2 fracturing fluid in petroleum engineering: A brief review. *Petroleum* **2024**, *10*, 1–10. [CrossRef]
38. Li, Q.; Wang, Y.; Wang, Y.; San, J.; Li, Q.; Foster, G. Synthetic process on hydroxyl-containing polydimethylsiloxane as a thickener in CO_2 fracturing and thickening performance test. *Energy Sources Part A Recovery Util. Environ. Eff.* **2018**, *40*, 1137–1143. [CrossRef]
39. Deng, B.; Yin, G.; Li, M.; Zhang, D.; Lu, J.; Liu, Y.; Chen, J. Feature of fractures induced by hydrofracturing treatment using water and L-CO_2 as fracturing fluids in laboratory experiments. *Fuel* **2018**, *226*, 35–46. [CrossRef]
40. Yang, S.; Yu, Q. The role of fluid-rock interactions in permeability behavior of shale with different pore fluids. *Int. J. Rock Mech. Min. Sci.* **2022**, *150*, 105023. [CrossRef]
41. Ouyang, L. New correlations for predicting the density and viscosity of supercritical carbon dioxide under conditions expected in carbon capture and sequestration operations. *Open Pet. Eng. J.* **2011**, *5*, 132–156. [CrossRef]
42. Klatte, D. On a Frank-Wolfe type theorem in cubic optimization. *Optimization* **2019**, *68*, 539–547. [CrossRef]
43. Sun, N.; Gao, M.; Liu, J.; Zhao, G.; Ding, F.; You, Q.; Dai, C. A novel temperature-resistant fracturing fluid for tight oil reservoirs: CO_2-responsive clean fracturing fluid. *Colloids Surf. A Physicochem. Eng. Asp.* **2023**, *665*, 131247. [CrossRef]
44. Li, C.; Huang, Y.; Sun, X.; Gao, R.; Zeng, F.B.; Tontiwachwuthikul, P.; Liang, Z. Rheological properties study of foam fracturing fluid using CO_2 and surfactant. *Chem. Eng. Sci.* **2017**, *170*, 720–730. [CrossRef]
45. Li, Q.; Wang, F.; Wang, Y.; Zhang, J.; Yu, X.; Zhao, M.; Zhou, C.; Forson, K.; Shi, S.; Zhao, Y.; et al. Influence of organoboron cross-linker and reservoir characteristics on filtration and reservoir residual of guar gum fracturing fluid in low-permeability shale gas reservoirs. *Environ. Sci. Pollut. Res.* **2022**, *29*, 82975–82985. [CrossRef]
46. Cong, Z.; Li, Y.; Pan, Y.; Liu, B.; Shi, Y.; Wei, J.; Li, W. Study on CO_2 foam fracturing model and fracture propagation simulation. *Energy* **2022**, *238*, 121778. [CrossRef]
47. Sun, B.; Sun, W.; Wang, H.; Li, Y.; Fan, H.; Li, H.; Chen, X. Molecular simulation aided design of copolymer thickeners for supercritical CO_2 as non-aqueous fracturing fluid. *J. CO_2 Util.* **2018**, *28*, 107–116. [CrossRef]
48. Sun, W.; Wang, H.; Zha, Y.; Yu, J.; Zhang, J.; Ge, Y.; Sun, B.; Zhang, Y.; Gao, C. Experimental and microscopic investigations of the performance of copolymer thickeners in supercritical CO_2. *Chem. Eng. Sci.* **2020**, *226*, 115857. [CrossRef]
49. Wang, X.; Hao, F.; Xu, H.; Zhu, C.; Jiang, T.; Jiang, Y. Static expansion fracturing mechanism for enhancing gas permeability in low permeability coal seams. *Sci. Rep.* **2024**, *14*, 25046. [CrossRef] [PubMed]
50. Jiang, C.; Wang, Y.; Duan, M.; Guo, X.; Chen, Y.; Yang, Y. Experimental study on the evolution of pore-fracture structures and mechanism of permeability enhancement in coal under cyclic thermal shock. *Fuel* **2021**, *304*, 121455. [CrossRef]
51. Bagherzadeh, P.; Goshtasbi, K.; Kazemzadeh, E.; Kashef, M.; Aloki Bakhtiari, H. Stress-dependence of the permeability, porosity, and compressibility in fractured porous media regarding fracturing condition. *Bull. Eng. Geol. Environ.* **2021**, *80*, 5091–5110. [CrossRef]

52. Wang, Z.; Sun, B.; Sun, X. Calculation of temperature in fracture for carbon dioxide fracturing. *SPE J.* **2016**, *21*, 1491–1500. [CrossRef]
53. Li, Q.; Li, Q.; Wang, F.; Wu, J.; Wang, Y. The carrying behavior of water-based fracturing fluid in shale reservoir fractures and molecular dynamics of sand-carrying mechanism. *Processes* **2024**, *12*, 2051. [CrossRef]
54. Li, Q.; Wang, F.; Wang, Y.; Bai, B.; Zhang, J.; Lili, C.; Sun, Q.; Wang, Y.; Forson, K. Adsorption behavior and mechanism analysis of siloxane thickener for CO_2 fracturing fluid on shallow shale soil. *J. Mol. Liq.* **2023**, *376*, 121394. [CrossRef]
55. Downs, R.T.; Gibbs, G.V.; Bartelmehs, K.L.; Boisen, M.B. Variation of bond lengths and volumes of silicate tetrahedra with temperature. *Am. Mineral.* **1992**, *77*, 751–757.
56. Liu, F.; Song, Q.; Zhang, N.; Bao, J.; Chen, Y. The influence of fracturing fluid temperature and viscosity on the migration and distribution of proppants within a fracture. *J. Pet. Explor. Prod. Technol.* **2024**, *14*, 3145–3159. [CrossRef]
57. Barati, R.; Liang, J.T. A review of fracturing fluid systems used for hydraulic fracturing of oil and gas wells. *J. Appl. Polym. Sci.* **2014**, *131*, 40735. [CrossRef]
58. Meng, Y.; Li, Z.; Lai, F. Evaluating the filtration property of fracturing fluid and fracture conductivity of coalbed methane wells considering the stress-sensitivity effects. *J. Nat. Gas Sci. Eng.* **2020**, *80*, 103379. [CrossRef]
59. Luo, Z.; Wu, L.; Zhao, L.; Zhang, N.; Chen, W.; Liang, C. Numerical study on filtration law of supercritical carbon dioxide fracturing in shale gas reservoirs. *Greenh. Gases Sci. Technol.* **2021**, *11*, 871–886. [CrossRef]
60. Brown, I.D.; Klages, P.; Skowron, A. Influence of pressure on the lengths of chemical bonds. *Acta Crystallogr. Sect. B Struct. Sci.* **2003**, *59*, 439–448. [CrossRef] [PubMed]
61. Devine, R.A.B.; Arndt, J. Si—O bond-length modification in pressure-densified amorphous SiO_2. *Phys. Rev. B* **1987**, *35*, 9376. [CrossRef] [PubMed]
62. Zhang, X.; Wang, J.G.; Gao, F.; Ju, Y. Impact of water, nitrogen and CO_2 fracturing fluids on fracturing initiation pressure and flow pattern in anisotropic shale reservoirs. *J. Nat. Gas Sci. Eng.* **2017**, *45*, 291–306. [CrossRef]
63. Li, Q.; Li, Q.; Wu, J.; Li, X.; Li, H.; Cheng, Y. Wellhead Stability during Development Process of Hydrate Reservoir in the Northern South China Sea: Evolution and Mechanism. *Processes* **2025**, *13*, 40. [CrossRef]
64. Belousov, A.; Lushpeev, V.; Sokolov, A.; Sultanbekov, R.; Tyan, Y.; Ovchinnikov, E.; Shvets, A.; Bushuev, V.; Islamov, S. Hartmann–Sprenger Energy Separation Effect for the Quasi-Isothermal Pressure Reduction of Natural Gas: Feasibility Analysis and Numerical Simulation. *Energies* **2024**, *17*, 2010. [CrossRef]
65. Bondarenko, A.V.; Islamov, S.R.; Ignatyev, K.V.; Mardashov, D.V. Laboratory studies of polymer compositions for well-kill under increased fracturing. *Perm J. Pet. Min. Eng.* **2020**, *20*, 37–48. [CrossRef]
66. Mardashov, D.; Nefedov, Y.; Islamov, S. Specifics of well killing technology during well service operation in complicated conditions. *Period. Tche Quim.* **2020**, *17*, 782–792. [CrossRef]
67. Islamov, S.R.; Bondarenko, A.V.; Korobov, G.Y.; Podoprigora, D.G. Complex algorithm for developing effective kill fluids for oil and gas condensate reservoirs. *Int. J. Civ. Eng. Technol.* **2019**, *10*, 2697–2713.
68. Zhao, H.; Wu, K.; Huang, Z.; Xu, Z.; Shi, H.; Wang, H. Numerical model of CO_2 fracturing in naturally fractured reservoirs. *Eng. Fract. Mech.* **2021**, *244*, 107548. [CrossRef]
69. Wang, L.; Yao, B.; Xie, H.; Winterfeld, P.H.; Kneafsey, T.J.; Yin, X.; Wu, Y.S. CO_2 injection-induced fracturing in naturally fractured shale rocks. *Energy* **2017**, *139*, 1094–1110. [CrossRef]
70. Wang, J.; Wang, Z.; Sun, B.; Gao, Y.; Wang, X.; Fu, W. Optimization design of hydraulic parameters for supercritical CO_2 fracturing in unconventional gas reservoir. *Fuel* **2019**, *235*, 795–809. [CrossRef]
71. Zou, Y.; Li, S.; Ma, X.; Zhang, S.; Li, N.; Chen, M. Effects of CO_2–brine–rock interaction on porosity/permeability and mechanical properties during supercritical-CO_2 fracturing in shale reservoirs. *J. Nat. Gas Sci. Eng.* **2018**, *49*, 157–168. [CrossRef]

Disclaimer/Publisher's Note: The statements, opinions and data contained in all publications are solely those of the individual author(s) and contributor(s) and not of MDPI and/or the editor(s). MDPI and/or the editor(s) disclaim responsibility for any injury to people or property resulting from any ideas, methods, instructions or products referred to in the content.